World Applied Sciences Journal 12 (9): 1505-1511, 2011
ISSN 1818-4952


# Effect of Thermal Treatment on the Morphology of ZnS:Mn Nanocrystals

*[2]Mohammad Syuhaimi Ab-Rahman, [2,3]Noor Azie Azura Mohd Arif and [1]Sahbudin Shaari*

[1]Institute of Micro Engineering and Nanoelectronics, Faculty of Engineering and Built Environment, National University of Malaysia, 43600 UKM Bangi, Selangor, Malaysia
[2]Computer and Network Security Research Group, Department of Electrical, Electronics and Systems Engineering, Faculty of Engineering and Built Environment, National University of Malaysia, 43600 UKM Bangi, Selangor, Malaysia
[3]Centre for Pre University, Universiti Malaysia Sarawak, 94300 Kota Samarahan, Kuching, Sarawak, Malaysia

**Abstract:** The arrangement, structure and formation of nanocrystals depend on the thermal treatment. This work focuses on the influences of the thermal treatment of manganese-doped zinc sulphide (ZnS:Mn) nanocrystals on their self-arrangement. A film was prepared by the sol gel method and layered by spin coating after 48 hours of stirring. We have found that a nanocrystalline layer of good quality can be obtained if a longer annealing treatment is applied.

**Key words:** ZnS:Mn · Nanocrystals · Sol gel method · Thermal treatment

## INTRODUCTION

Recently, several physical and chemical methods have been used for the fabrication of nanocrystals [1-20]. The development of good nanocrystals with well-aligned morphology is impacted by many factors such as the reactant, concentration, solvent, temperature, interactions between nanoparticles and reaction time [1-7, 20-26]. Some studies reported that the thermal stability of nanocrystalline materials affected the formation of nanocrystals. Thus, the study of nanocrystal thermal stability has been an urgent issue from the viewpoint of practical applications and theoretical research. Here, we developed a convenient sol gel approach assisted by a self-assembly technique for the synthesis of ZnS:Mn nanocrystals. The physical characteristics of ZnS:Mn such as surface properties was determined. The prepared nano ZnS: Mn material was characterized by energy dispersive x-ray (EDX) spectroscopy, UV-Vis spectrometry (Perkin Elmer Lambda 35) and field emission scanning electron microscopy (FE-SEM).

**Experimental Part:** Mn-doped ZnS nanocrystals were synthesized by a self-assembly technique through the sol-gel method. To prepare nanocrystals of ZnS:Mn, zinc nitrate hexahydrate and manganese acetate were dissolved in a solution of 2-propanol and distilled water. Then, thiourea was added to this solution as the source of sulphur. The solution was mixed using a magnetic stirrer at 300 rpm. After 48 hours of stirring, a clear and transparent sol was obtained. Then, the films were prepared by spin coating on glass slide substrates. Two coated thin film samples were heated from room temperature to 300°C at 3°C/min and 0.5°C/min ramping rates. Afterwards, the thin films remained at the peak temperature for 60 minutes before ramping down at the normal rates. The thin film layers were then inspected under FE-SEM with 3 kV electron energy to determine the morphology of the Mn-doped ZnS in the as-delivered condition. The FE-SEM micrographs displayed rounded particles with a relatively homogeneous and inhomogeneous size distribution.

## RESULTS AND DISCUSSION

**Optical Properties and Morphology of Nanocrystals after the Annealing Process:** The optical properties of the ZnS:Mn nanocrystalline thin films were determined from transmittance and absorbance measurements in the range of 200-1000 nm. Fig. 1 shows the transmission and absorption spectra of nanocrystalline ZnS:Mn thin films.

**Corresponding Author:** Noor Azie Azura Mohd Arif, Computer and Network Security Research Group, Department of Electrical, Electronics and Systems Engineering, Faculty of Engineering and Built Environment, National University of Malaysia, 43600 UKM Bangi, Selangor, Malaysia.
E-mail: azie@vlsi.eng.ukm.my & manaazura@preuni.unimas.my.

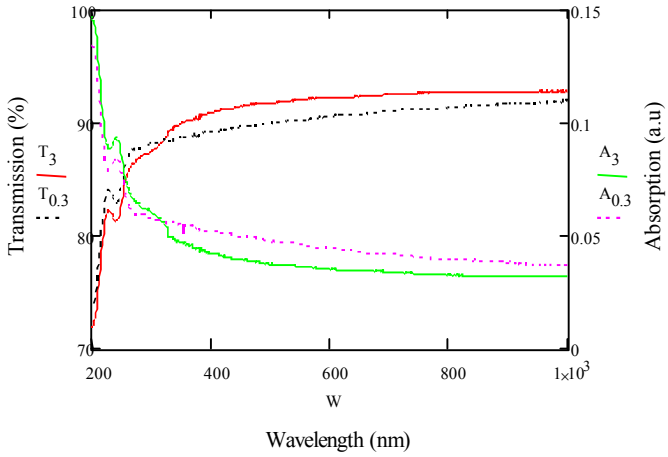


Fig. 1: Transmission and absorption spectra for different annealing treatment

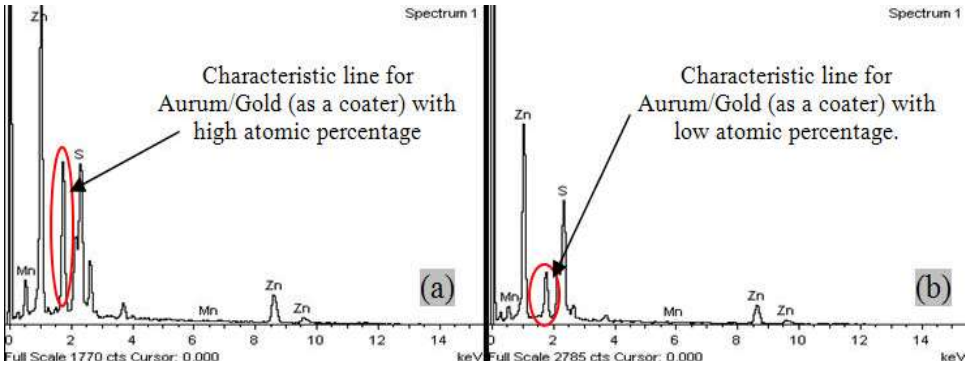


Fig. 2: Representative energy dispersive X-ray spectrum for ZnS:Mn nanocrystals with different thermal treatments

The results for both conditions show an optical transmittance over of 88% in the visible region. ZnS has good absorption for light in the wavelength of range 220 nm-350 nm as shown in Fig. 1. In same figure, it can be seen that the strongest absorption peak of the as-prepared sample appears at around 250 nm, which is fairly blue shifted from the absorption edge of the bulk ZnS (345 nm). This shift is due to the quantum confinement effect as mentioned by Sarkar *et al.* [29]. The longer-duration clearly has high absorption in the absorption graph, while it has a lower transmission percentage in the transmission graph.

Figure 2 shows the elemental concentration of the samples, confirming the composition of Mn-doped ZnS. The EDX analysis shows high intensity peaks assigned to elemental zinc (Zn), sulphur (S) and manganese (Mn) characteristics lines. The atomic percentages were found to be 67.55 %, 28.50 % and-, 3.95 % (0.5°C/min) and 65.33%, 26.84% and-, 7.83% (3.0°C/min) respectively. In Fig. 2a, the atomic percentage of silicon (as a substrate) is high compared to that in Fig. 2b because the surface on the substrate was not fully filled with ZnS:Mn nanocrystals. In other words, the morphology of the nanocrystals was not well aligned.

The FESEM image in Fig. 3 demonstrates the optimum growth conditions at a relatively low annealing temperature of Mn-doped ZnS nanocrystals. The high magnification FESEM images reveals that the product consists of nano-sized spherical particles with nanocrystals formed in a range of 15-30 nm. The annealing temperature affects the configurations of the nanocrystals for both samples. When the reaction annealing time is fast (8 hrs), the crystallization of the product is poor and the particles are not properly aligned, some particles agglomerate to a great extent. The interstitials space is also not completely filled. On the hand, at the longer annealing time (41 hrs), the Mn-doped ZnS nanocrystals are clearly well aligned. The annealing temperature duration is an important factor for the morphological evolution of the structures. The shorter annealing duration does not favor uniform nanocrystals. Furthermore, the product obtained with the shorter duration is the aggregation of inhomogeneous nanocrystals as shown in Fig. 3a and 3b.

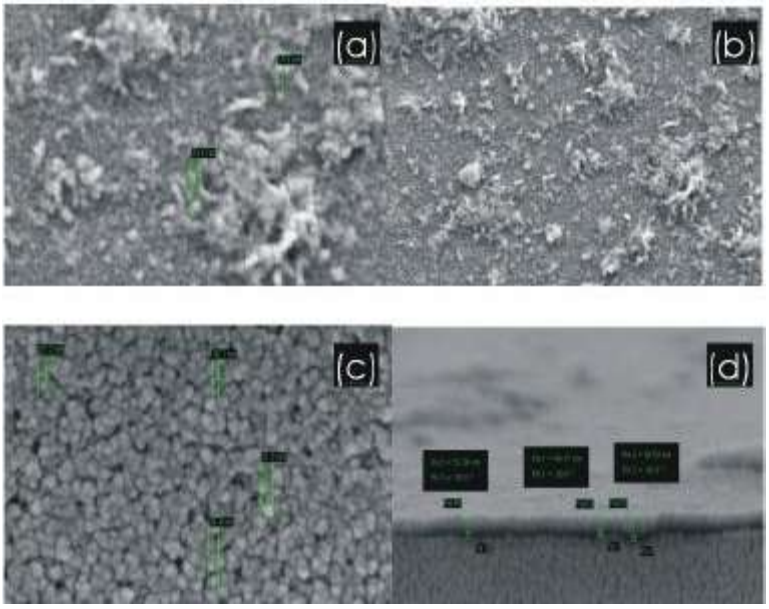


Fig. 3: (a) High and (b) low magnification FESEM images of the ZnS:Mn nanocrystals generated with the shorter annealing duration (c) FESEM image for the longer annealing duration (d) cross sectional surface for the longer annealing duration.

In contrast, the sample synthesized at a longer duration is composed of relatively uniform nanocrystals with diameters of several nanometers. With short annealing times, the crystallization process is expected to be fast, which is critical for the control of the reduction kinetics. Therefore the size of the nanoparticles can be expected to be inhomogeneous. Hence, it is difficult to form a layer with good nanocrystals arrangement. For the sample with longer duration annealing however, the crystallization process is slow and fully under control, so the results are more uniform and more homogeneous.

The thin film layer is clearly defined as shown in Fig. 3d. The intense thermal treatment with longer annealing time improves the reaction efficiency and crystallinity. Therefore, the amount of thermal energy received by the nanocrystals is sufficiently high for atomic re-ordering or agglomeration effects. Based on the mechanism of crystallization, the kinetics of the transition and chemical reactions are related to the annealing temperature, which is recognized as a primary factor for the promotion of crystallization.

In this work, the formation and self-assembly of Mn-doped ZnS nanocrystals mainly occurred via three steps. At the initial stage, ZnS:Mn was formed, leading to the formation of many primary nanocrystals. The nanocrystals had a low kinetic energy due to translational kinetic energy and the internal energy of each particle (rotational and vibrational kinetic energy). Under high temperature, the nanocrystals had more motion due to the high energy. The movement was random and not a static vibration as in the first step. At the initial stage, atoms were held close to each other and vibrated, but they stayed in close proximity. However, in this stage, the kinetic energy of the atoms was greater and thus they were much further apart and more free of each other. During cooling time, the energy decreased. In this stage, only reorientation of random atoms or the atomic arrangement of ZnS:Mn nanocrystals might occur in the system. The ZnS:Mn nanocrystals attached side-by-side to self assemble. A schematic illustration of the development of self-assembled ZnS:Mn nanocrystals is shown in Fig. 4.

**Kinetics and Potential Energy of Nanocrystalline ZnS:Mn the During Annealing Process:** Nanocrystal arrangements within a drop of dilute ZnS:Mn nanocrystals on glass slides formed spontaneously after spin coating process. However, the actual arrangement resulted from the heat treatment process. In the thermal process, the formation of alignments can be modelled as a gas system. The motion of the nanocrystals can be controlled by the total energy in the system, which is the sum of the kinetic and potential energies. Hence, a general total energy, *E(T)* dependence on temperature during the process can be obtained by:

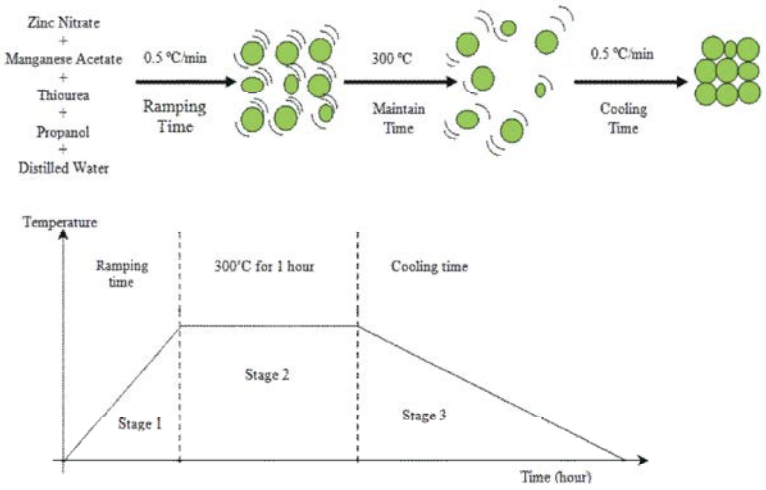


Fig. 4: Schematic illustration of the mechanism of formation of the Mn doped ZnS nanocrystals

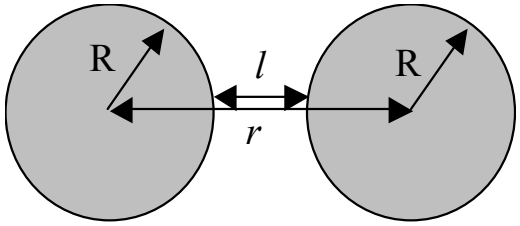


Fig. 5: R is the radius, r is the distance from both centres of the nanocrystals and l is the distance between nanocrystals.

$$E(T) = KE(T) + PE(T) \tag{1}$$

where *KE(T)* is the kinetic energy and *PE(T)* is the potential energy. The kinetic energy form can be written as Eq. 2:

$$KE(T) = \frac{3}{2} k_B T \tag{2}$$

where the equation is equal to the kinetic energy of the electron, (1/2)*mnVth 2* (30). Here, *kB* is the Boltzmann constant, *T* is the temperature in Kelvin, *Vth* is the thermal velocity and *mn* is the electron effective mass. The potential energy is derived from van der Waals attraction [27]. Normally, this force has three different types: Keesom interactions, Debye interactions and London interactions [28]. In this case, however, the Keesom interaction is considered because it occurs between molecules with permanent dipoles. ZnS:Mn nanocrystals have permanent dipole forces in the covalent bond, resulting in the sharing of a pair of electrons. The Keesom interaction is expressed as follows:

$$PE(T) = -\frac{1}{r^6} \frac{2\mu_1^2 \mu_2^2}{(4\varepsilon\pi)^6 (3k_B T)} \tag{3}$$

Here *r* is the distance from the centres of both nanocrystals, μ is the dipole moment of each molecule and *å* is the dielectric constants. Fig. 5 shows the schematic representation of two nanocrystals labeled with the parameters.

Based on Eq. 2 and Eq. 3, the kinetic and potential energy dependences on the temperature are plotted in Fig. 6 and Fig. 7. Specifically, if the nanocrystals are in the static position, the system has potential energy as in the first stage. The kinetic energy is less than 250 x $10^{-23}$ J because of the thermal energy in the system at room temperature. When the system is heated, the nanocrystals are free to move and this potential energy is converted into kinetic energy. The nanocrystals increase their speed as they move into the potential 'well', reaching maximum kinetic energy when they reach the minimum of the potential (near $T = 300°C$). The nanocrystals then stretch past the equilibrium position and the energy increases again until it equals its initial value. During this cooling time, the nanocrystal motion decreases and at the same time, the nanocrystals experience stronger attraction due to screening of the van der Waals force between them. Fig. 8 shows the kinetic and potential energies during the annealing process, these energies mirror each other because their sum, the total energy, should remain constant.

To further investigate the effect of temperature ramping rate with time, we consider the kinetic energy dependence on time as:

$$KE(t) = \sum_{j=1}^{t} \frac{3}{2} k_B (nt) \tag{4}$$

for the initial stage. In the final stage, kinetic energy becomes:

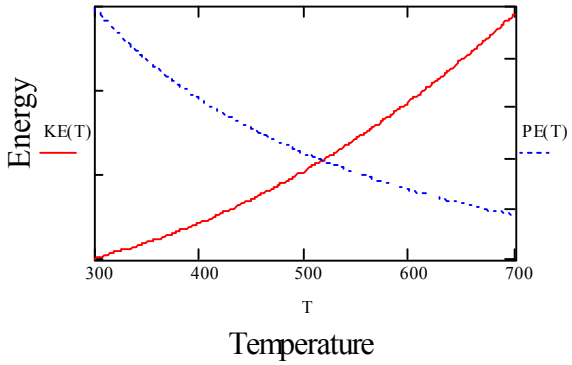


Fig. 6: The kinetic and potential energy dependence on temperature for the first stage.

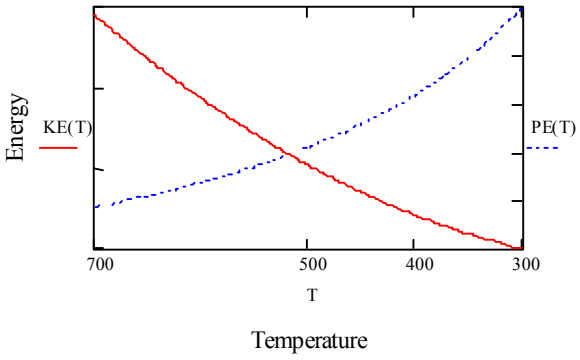


Fig. 7: The kinetic and potential energy dependence on temperature for the final stage.

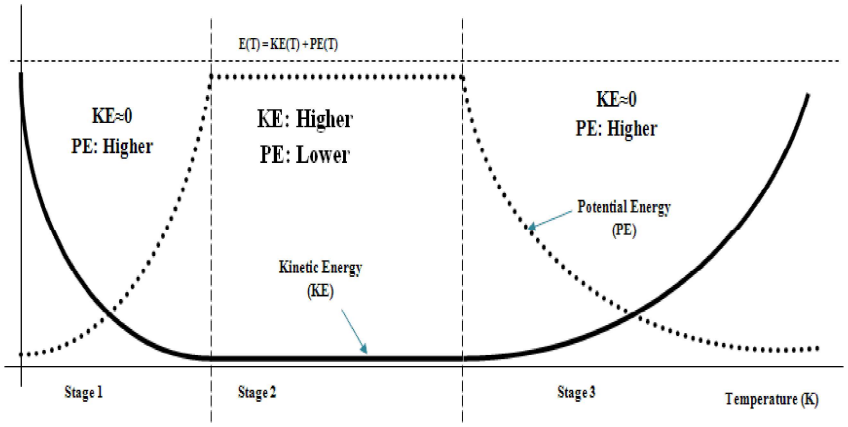


Fig. 8: The kinetic and potential energy during the annealing process

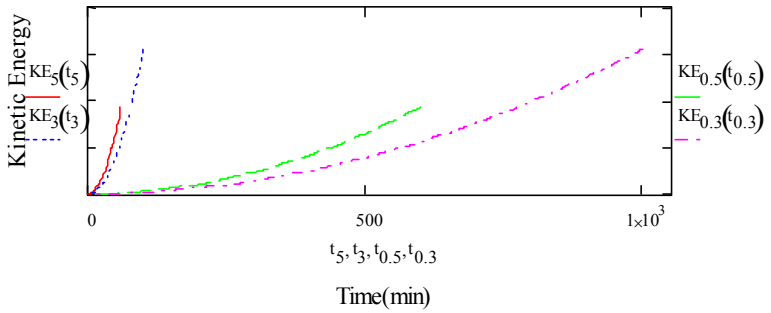


Fig. 9: The kinetic energy for the first stage with different temperature ramping rate effects.

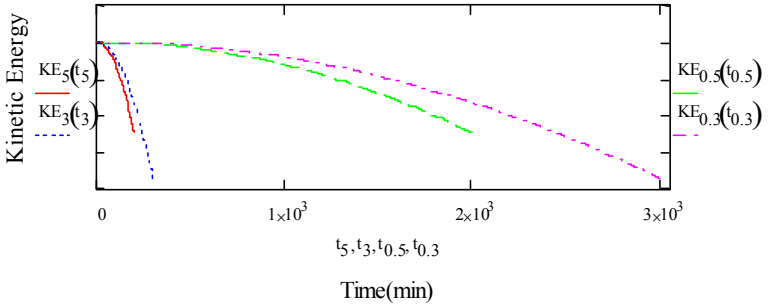


Fig. 10: The kinetic energy for the final stage with different temperature ramping rate effects.

$$KE(t) = \left(\frac{3}{2}k_B T\right) - \sum_{j=1}^{t} \frac{3}{2}k_B (nt) \quad (5)$$

where $t$ is the time, $T$ is the temperature and $n$ is the temperature ramping rate. Graphs with different temperature ramping rates ($n$ = 5°C/min, 3°C/min, 0.5°C/min and 0.3°C/min) are plotted in Fig. 9 and Fig. 10. In both of the graphs, when the temperature ramping rate is lower, a longer duration is required to reach 300°C and then cool down to room temperature. Hence, nanocrystal arrangement can be better when a lower temperature ramping rate is applied due to the crystallization process in stage 3, in which the process is fully under control during slow ramping in contrast to the lack of control observed with faster ramping. A similar result can be obtained for the potential energy dependence on time by using different temperature ramping rates.

## CONCLUSIONS

In this work, the effects of thermal treatment during the formation of a Mn-doped ZnS nanocrystal system were studied as a determinant factor in the self-assembly mechanism after deposition. It was shown in a standard synthesis procedure that depending on the heating temperature duration, it is possible to achieve well-organized arrays or agglomerates. The quality increases with increasing duration at slow ramping rate. Thus, the longer annealing time was found to be sufficient to produce ZnS:Mn nanoparticles thin film layers of good quality using the sol gel method through the self assembly fabrication technique.

## ACKNOWLEDGEMENTS

We are grateful to the Universiti Kebangsaan Malaysia Research University Grant for the support of this research.

## REFERENCES

1. Concustell, A., G. Alcala, S. Mato, T.G. Woodcock, A. Gebert, J. Eckert and M.D. Baro, 2005. Effect of Relaxation and Primary Nanocrystallization on The Mechanical Properties of $Cu_{60}Zr_{22}Ti_{18}$ Bulk Metallic Glass. Intermetallics, 13: 1214-1219.
2. Mondal, K., T. Ohkubo, T. Toyama, Y. Nagai, M. Hasegawa and K. Hono, 2008. The Effect of Nanocrystallization and Free Volume on The Room Temperature Plasticity of Zr-based Bulk Metallic Glasses. Acta Materiallia, 56: 5329-5339.
3. Kuenle, M., S. Janz, O. Eibl, C. Berthold, V. Presser and K.G. Nickel, 2009. Thermal Annealing of SiC Thin Films With Varying Stoichiometry. Materials Science and Engineering, 159-160: 355-360.
4. Wei, D., W. Qian, Y. Shi, S. Ding and Y. Xia, 2008. Effect of Cooling Treatment and Glutaradehyde on The Morphology of Au Nanostructures Synthesized From Chitosan. Carbohydrate Research, 343: 512-520.
5. Simeonidis, K., S. Mourdikoudis, I. Tsiaoussis, C.D. Samara, M. Angelakeris and O. Kalogirou, 2008. Thermal Treatment Effects In The Self-assembly of FePt Nanoparticle Arrays. Jounal of Magnetism and Magnetic Materials, 320: 2665-2671.
6. Zhang, W., S. Zhang, Y. Liu and T. Chen, 2009. Evoluton of Si Suboxides Into Si Nanocrystals During Rapid Thermal Annealing As Revealed by XPS and Raman Studies. Journal of Crystals Growth, 311: 1296-1301.
7. Wang, C., E. Shen, E. Wang, L. Gao, Z. Kang, C. Tian, Y. Lan and C. Zhang, 2005. Controllable Synthesis of ZnO Nanocrystals Via A Surfactant-assisted Alcohol Thermal Process At A Low Temperature. Materials Letters, 59: 2867-2871.
8. Borah, J.P. and K.C. Sarma, 2008. Optical and Optoelectronic Properties of ZnS Nanostructured Thin Film, Acta Physica Polonica, A., 114: 713-719.
9. Bhattacharjee, B., D. Ganguli, K. Iakoubovskii, Stesmans and S. Chaudhari, 2002. Synthesis and Characterization of Sol-gel Derived ZnS: Mn Nanocrystallites Embedded In A Silica Matrix, Bull. Mater. Sci., 25: 175-180.
10. Bhattacharjee, B., D. Ganguli, S. Chaudhari and A.K. Pal, 2002. ZnS:Mn Nanocrystallites in $SiO_2$ Matrix: Preparation And Properties, Thin Solid Film, 422: 98-103.
11. Ghosh, S.C., C. Thanachayanont and J. Dutta, 2004. Studies on Zinc Sulphide Nanoparticles for Field Emission Devices, ECTI-CON, pp: 145-148.
12. Murali, K.R., J. Abirami and T. Balasubramanian, 2008. Pulse plated zinc sulphide films and their characteristics. J. Mater Sci: Mater Electron., 19: 217-222.
13. Ubale, A.U. and D.K. Kulkarni, 2005. Preparation and study of thickness dependent electrical characteristics of zinc sulfide thin films. Bull. Mater. Sci., 28: 43-47.
14. Murugan, A.V., O.Y. Heng, V. Ravi, A.K. Viswanath and V. Saaminathan, 2006. Photoluminescence properties of nanocrystalline ZnS on nanoporous silicon. J. Mater Sci., 41: 1459-1464.

15. Hebalkar, N., A. Lobo, S.R. Sainkar, S.D. Pradhan, W. Vogel, J. Urban and S.K. Kulkarni, 2001. Properties of zinc sulphide nanoparticles stabilized in silica. J. Materials Sci., 36: 4377-4384.
16. Devi, B.S.R., R. Rveendran and A.V. Vaidyan, 2007. Synthesis and Characterization of Mn Doped ZnS Nanoparticles, Journal of Physics, 68: 679-687.
17. Yoon, K.H., J.K. Ahn and J.Y. Cho, 2001. Optical Characteristics of Undoped and Mn Doped ZnS Films, J. Materials Sci., 36: 1373-1376.
18. Yang, H., J. Zhao, L. Shen, L. Song, Z. Wang, L. Wang and D. Zhang, 2003. Photoluminescence Properties of ZnS:Mn Nanocrystals Prepared In Inhomogeneous System. Materials Letters, 57: 2287-2291.
19. Chang, X., J. Cao, H. Ji, B. Fang, J. Feng, L. Pan, F. Zhang and H. Wang, 2005. Solvothermal Synthesis of 3D Photonic Crystals Based on ZnS/Opal System, Materials Chemistry and Physics, 85: 6-10.
20. Mingzhi, W., X. Shifang, Y. Xiaojian and H. Wangyu, 2006. Molecular Dynamics Simulation of Thermal Stability of Nanocrystalline Vanadium. Sci. China E-Technol. Sci., 49: 400-407.
21. Yang, L.X., Y.J. Zhu, H. Tong and W.W. Wang, 2007. Submicrocubes And Highly Oriented Assemblies of MnCO3 Synthesized By Ultrasound Agitation Method And Their Thermal Transformation To Nanoporous $Mn_2O_3$, Ultrasonics Sonochemistry, 14: 259-265.
22. Khaodee, W., B. Jongsomjit, P. Praserthdam, S. Goto and S. Assabumrungrat, 2008. Impact Of Temperature Ramping Rate During Calcinations On Characteristics Of Nano-$ZrO_2$ And Its Catalytic Activity For Isosynthesis, Journal of Molecular Catalysis A: Chemical, 280: 35-42.
23. Xiao, Z.L., E.Y. Andrei, Shuk and M. Greenblatt, 2000. Current Ramping Rate Dependence of The Critical Current In 2H-NbSe 2 Crystals. Physica C., 341-348: 1163-1164.
24. Steitz, B., Y. Axmann, H. Hofmann and A.P. Fink, 2008. Optical Properties of Annealed $Mn^{2+}$ Doped ZnS Nanoparticles. Journal of Luminescence, 128: 92-98.
25. Li, J., J. Zhang and Y. Qian, 2008. Surfactant-assisted Synthesis of Bundle-like Nanostructures With Well-aligned Te Nanorods. Solid State Sciences, 10: 1549-1555.
26. Isabelle Lisiecki, 2004. Size Control of Spherical Metallic Nanocrystals. Colloids and Surfaces A: Physicochem, Eng. Aspects, 250: 499-507
27. Sarkar, R., C.S. Tiwary, P. Kumbhakar and S. Basu, 2008. Yellow-orange Light Emission From $Mn^{2+}$ Doped ZnS Nanoparticles, Physica, E., 40: 3115-3120.
28. Arora, V.K., 2000. Quantum Engineering of Nanoelectronic Devices: The Role of Quantum Emission in Limiting Drift Velocity And Diffusion Coefficient, Microelectronics Journal, 31: 853-859.
29. Adrian, P., 0000. Van der Waals Forces: A Handbook for Biologists, Chemists, Engineers and Physicists V, (to be published).
30. Yoo, S.L., 2008. Self-Assembly and Nanotechnology A Force Balance Approach, A John Wiley and Sons, Inc., pp: 3-33.